# ADVANCED SURFACE CLEANING METHODS -THREE YEARS OF EXPERIENCE WITH HIGH PRESSURE ULTRAPURE WATER RINSING OF SUPERCONDUCTING CAVITIES- *

P. KNEISEL and B. LEWIS

*Continuous Electron Beam Accelerator Facility*
*12000 Jefferson Avenue, Newport News, Virginia 23606 USA*

In the last three years we have carried out a large number of tests on single cell and multi-cell niobium and $Nb_3Sn$ cavities at L-band frequencies, which as a final surface cleaning step had been rinsed with high pressure jets of ultrapure water. This treatment resulted in an unprecedented quality and reproducibility of cavity performance. Field emission free surfaces up to peak surface electric fields of $E_{peak} \geq 45$ MV/m were achieved nearly routinely after buffered chemical polishing of niobium surfaces. In addition, residual surface resistances below $R_{res} \leq 10$ n$\Omega$ and as low as $R_{res} = 2$ n$\Omega$ were not uncommon. In 5-cell production cavities of the Cornell/CEBAF shape gradients as high as $E_{acc} = 21.5$ MV/m corresponding to peak surface fields of $E_{peak} \approx 55$ MV/m have been measured after post purification with Ti without the need for rf-processing. Several $Nb_3Sn$ - cavities exhibited no field emission loading after high pressure ultrapure water rinsing up to the maximum achievable surface fields of $E_{peak} \approx 33$ MV/m; the field limits were given by the available rf-power. The unprecedented reproducibility of the cavities permitted serial testing of various parameters effecting cavity performance such as the influence of residual gas inside the cavities prior to cooldown, the removal of the surface damage layer or the impact of peripheral parts such as rf-windows. The major portion of this paper summarizes several of the results obtained from investigations carried out during the last three years. The second part discusses possibilities for further improvements in cavity cleaning.

KEY WORD: Superconducting Cavities

## 1. INTRODUCTION

Since high purity niobium with RRR-values $\geq 250$ has become commercially available, superconducting niobium cavities used in particle accelerators are in most cases no longer limited in their performance by thermo-magnetic breakdown at defects at design accelerating gradients $E_{acc} \leq 8$ MV/m. However, in more ambitious projects such as the TTF[1] or possible upgrades of existing machines the gradient design goals are reaching or exceeding $E_{acc} \geq 15$ MV/m and the problem of thermal stabilization of defects needs to be address more seriously. In quite a large number of cases such high gradients have been reported in laboratory experiments, indicating that there does not seem to be a fundamental limit in achieving these goals. As a practical matter the principal limitations encountered at field levels above $\approx 8$ MV/m is field emission loading, characterized by exponentially increasing losses as the rf-field levels in the cavities are increased. This is especially true for more complex assemblies such as cavity pairs or cryomodules. Progress towards routinely achieving higher gradients for future applications of rf-superconductivity goes hand in hand with shifting the onset of field emission loading towards higher fields.

It is generally accepted that the field emission behavior of a niobium cavity reflects the level of cleanliness of the superconducting surfaces subject to the rf-fields. Artificial emitters introduced into the

cavities during surface treatments and assembly steps are the major causes for the emission of electrons. Emitters intrinsic to the material such as e.g. impurity segregation have only been identified after heat treatment at moderate temperatures. [2,3]

Three approaches or combinations of the three are presently practiced to eliminate field emission loading and to push achievable gradients to higher values:

a. ultrahigh vacuum annealing in the presence of a solid state gettering material such as titanium.[4,5]
b. high peak power rf-processing[6,7] and
c. advanced surface cleaning techniques such as high pressure rinsing[8-11] or megasonic agitation.[11]

In the cases of high temperature annealing and high peak power processing emitters clinging to the surfaces are destroyed. Both approaches are being applied successfully and accelerating gradients in excess of $E_{acc} \approx 20$ MV/m corresponding to surface electric fields of $E_{peak} \approx 40$ - 50 MV/m have been achieved in multi-cell cavities.[4-7]

The cleaning techniques mentioned in c. are applied to eliminate emitters from the surfaces prior to testing rather than destroying the emitters as happens during high peak power processing. These methods might be inherently advantageous, if one can avoid re-contamination of the surfaces during assembly steps. All production cavities at CEBAF receive a chemical polishing in a buffered solution of equal parts of hydrofluoric, nitric and phosphoric acids as a surface treatment followed by a thorough rinsing with ultrapure water. In some cases very exceptional cavity performances have been measured.[12] Three years ago we started a program to improve the final rinsing step in the chemical treatment procedure by directing a high pressure ultrapure water jet towards the niobium surfaces. Initial results were very encouraging and the procedure has been used rather routinely with very surprising reproducibility of cavity performance. This made it possible to conduct serial tests and study the influence of "environmental" conditions such as the cavity vacuum prior to cooldown, the thickness of the removed surface layer or Q-degradation as a function of metallurgical conditions on cavity performance as well as the impact of peripheral parts on cavity behavior.

In the following several results from our experience with high pressure rinsing of cavities under various "environmental" conditions are reported. In a final section the possibilities of further improvements in surface cleaning are reviewed.

## 2. THE HIGH PRESSURE RINSING SYSTEM

The high pressure rinsing system is schematically shown in Figure 1. It consists of a high pressure pump, a filter, a spray nozzle and a mechanical system, which allows the scanning of the interior surface with the high pressure water jet. Because of budgetary constraints and for exploratory testing we chose inexpensive components, which are by far not optimized: a commercial high pressure pump (Kärcher Model 1855-878) supplies approximately 8 liter of water per minute at 80 bar (at the filter inlet); the filter is a 0.1 μm cellulose filter (Domnick-Hunter "Asypor") rated for 80 bar and located in an unpolished stainless steel housing. Connecting lines are made of teflon with stainless steel braids; the spray nozzle and the rigid feedline from the filter to the spray nozzle are made of type 304 stainless steel. The scanning system moves the cavity up and down while also rotating it. Both up-and-down speed are adjustable by means of motors with variable speed controls.

For the majority of the experiments reported here we chose a rotational speed of ≈ 4 rpm and a vertical speed of ≈ 70 cm/min. Initially a "home-made" spray nozzle with four jets emerging under 45° (up and down) and 180° apart in azimuth as sketched in Figure 1 was used. This nozzle head was two years ago replaced with a spherical head with 12 jets equally spaced around the perimeter providing for a more uniform spray pattern during the cleaning operation. Single cell cavities were typically rinsed under these conditions for 20 min with ultrapure water with a resistivity of ≈ 18 MΩ cm; five cell cavities were rinsed for ≈ 60 min. Since the high pressure spray and the movement of the cavity seemed to create a low pressure inside the cavity, sucking in the dirty air from the chemical room where the rinsing system is located, all cavity openings were closed with teflon blank-offs and one of these covers had an air-filter attached to it. Prior to using the system for cavity cleaning it was operated for at least 15 min in order to rinse out possible contamination from sitting idle. The system–as mentioned above–was built for

exploratory tests and is far from being optimized: at the very least the high pressure pump should be made from stainless steel (our pump is probably made from cast iron) and the filter housing and connecting stainless steel parts should be polished. In addition the system should be incorporated in the ultrapure water polishing loop, thus avoiding areas of stagnant water and eliminating the danger of bacterial growth. A sampling port for particulate sampling or TOC–content sampling should be added at the downstream side of the filter and the high pressure rinsing should be performed in a better controlled, cleaner environment, preferably in the clean room. Despite of all these shortcomings the use of the present system was very beneficial and resulted in unprecedented reliability and reproducibility of cavity performance, which for one of us (PK) came as a pleasant surprise after many years of experimental work in superconducting cavity technology.

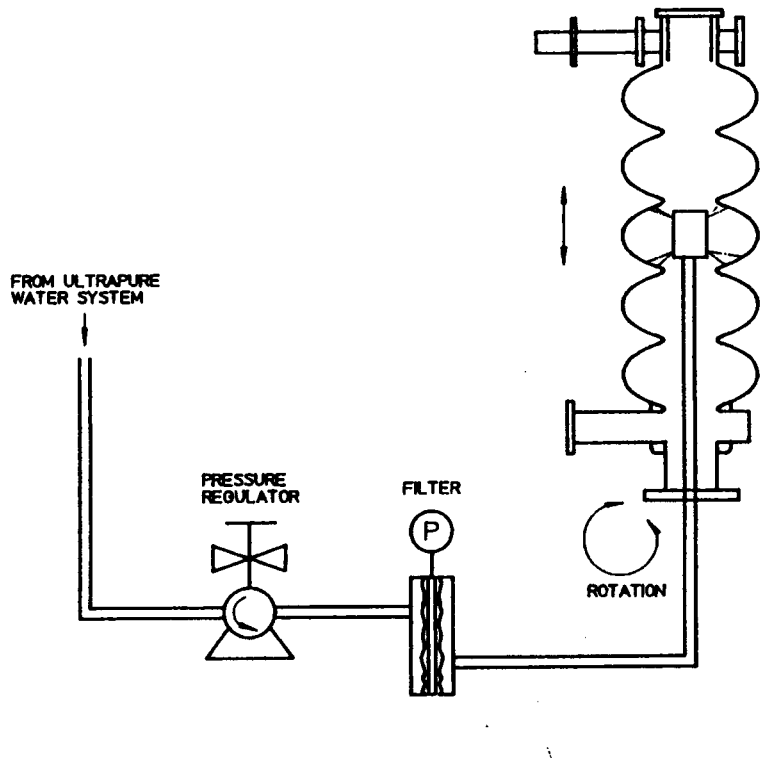


FIGURE 1: Schematic of high pressure rinsing system.

## 3. TEST PROCEDURES

Most of the more than 200 experiments carried out during the last 3 years have been done after applying consistently the same surface preparation treatment to the cavities: after initial fabrication with standard techniques such as deep drawing, machining and electron beam welding the cavities have been chemically polished in a buffered solution of equal parts of hydrofluoric, nitric and phosphoric acids after degreasing in a caustic solution with ultrasonic agitation. Afterwards the treated cavities were rinsed with the ultrapure high pressure water jets for an extended period of time prior to a final triple rinse with reagent grade methanol in our class 100 clean room. The assembly of peripheral parts such as rf–coupling probes or–in the case of 5-cell production cavities–ceramic rf-windows to the cavities followed after this rinsing step. Five cell cavities were attached to the cryogenic test set-up inside the clean room, single cell cavities had to be brought outside for mounting onto the test fixture. Typically the cavities were evacuated with a turbomolecular pump to a pressure better than $p \leq 10^{-5}$ torr; then the continuous pumping was switched over to an ion-pump. Once a vacuum of $\leq 10^{-6}$ torr was established in the cavity, it was cooled down to 4.2 K within less than 1 hour in an ambient magnetic field $\leq 5$ mGauss. Routinely the temperature of the helium bath was adjusted to 2 K and the cavity Q–value was measured as a function of rf–field in the cavity. Often the temperature dependence of the surface resistance was measured between 4.2 K and 2 K.

In several serial tests as mentioned below such as investigation of the effects of residual pressure inside the cavity prior to cooldown or the influence of peripheral parts such as rf–windows, the chemical polishing step was omitted after the initial "baseline" test and the cavities were only degreased, high pressure and methanol rinsed prior to subsequent assembly. As it turned out, this procedure resulted in consistently reproducible cavity performance and removed the possible ambiguities resulting from exposing a fresh niobium surface if buffered chemical polishing had to be applied.

## 4. EXPERIMENTAL RESULTS AND DISCUSSION

In the following we present experimental results, which will prove the reliability and the reproducibility of the treatment procedure described above. We credit this degree of cavity performance reproduction to the application of the high pressure ultrapure water rinsing, which made it afterwards possible to systematically look at the influence of various "environmental" conditions on cavity performance.

### *4.1 Reliability*

In Figure 2 experimental results of 4 different single cell cavities fabricated at different times from different materials are shown. All cavities reached or exceeded peak surface electric fields of $E_{peak} \geq 45$ MV/m with little or no field emission loading.

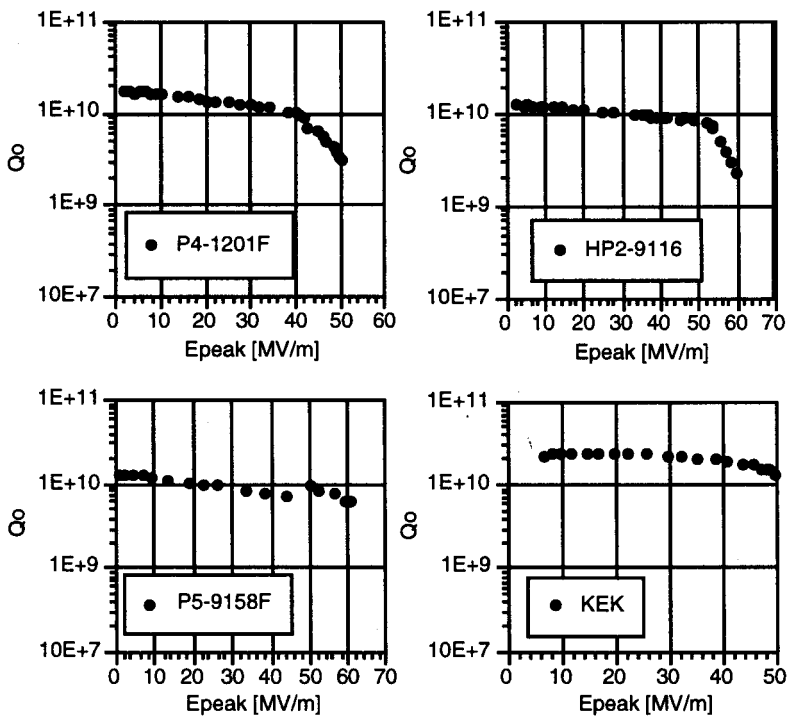


FIGURE 2: $Q_0$ vs. $E_{peak}$ at 2K for 4 different single cell cavities after high pressure ultrapure water rinsing. The KEK cavity has a frequency of 1300 MHz, all others are of the Cornell/CEBAF type operating at 1497 MHz

### *4.2 Reproducibility*

In Figure 3 results from a series of tests with the same cavity after successive buffered chemical treatments are shown. This particular cavity was during its life time post purified at 1400° C for 4 hours in the presence of titanium. The cavity was electropolished at KEK by K. Saito with the removal of 120 µm,

followed by a high pressure rinsing at KEK and shipment to CEBAF under vacuum. At CEBAF the cavity was disassembled in the clean room and rinsed with reagent grade methanol prior to the first test (see Figure 3, data were taken at 1.7K). Afterwards a high pressure rinsing was done at CEBAF, which resulted in an improved performance (also Figure 3). All other results shown in Figure 3 were measured after subsequent chemical polishing.

Results in Figure 3 are typical for sets of experiments done with different cavities. After the removal of the surface damage layer (see Section 4. 3) reproducible results were obtained after additional polishing steps.

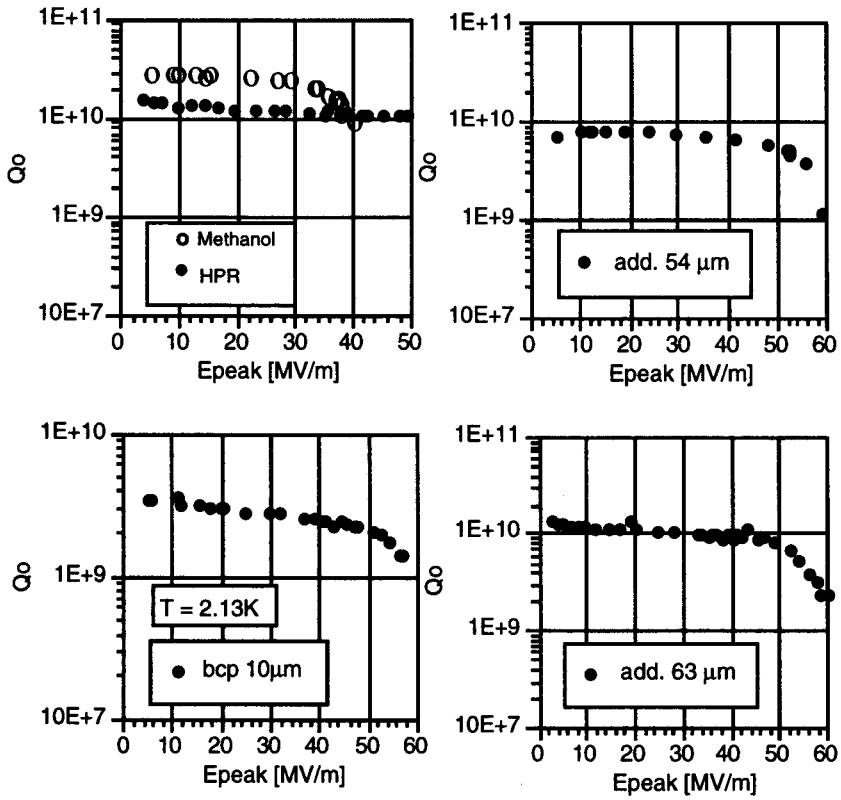


FIGURE 3: $Q_0$ vs. $E_{peak}$ after subsequent chemical polishing treatments of the same cavity.

### *4.3 Removal of Surface Damage Layer*

On several cavities successive steps of material removal through chemical polishing with subsequent measurements of the cavity performance were carried out. The objective of these tests were both to find out the minimal amount of damage layer removal necessary for good cavity performance and to get some information about the possibility of intrinsic field emission sites in the material.[13] The experimental results as shown in Figure 4 for one cavity indicate that CEBAF's standard removal thickness of 60–80 µm might have been somewhat on the low side and that better cavity performances can be achieved by removing more material. These test series also indicated that electron emitters are unlikely intrinsic to the material– additionally these experiments were accompanied by sample measurements on field emission samples as reported in[13] - but that defects in the damage layer are limiting cavity performance. In all tests shown in Figure 4 the cavity was limited by thermal magnetic breakdown in the absence of field emission loading. Figure 5 summarizes the results shown in Figure 4: according to these measurements high Q-values corresponding to small residual resistance values can be achieved after the removal of approximately 60 µm whereas it is beneficial for higher gradients to remove at least twice as much material from the surface. Very similar results have been reported in[14].

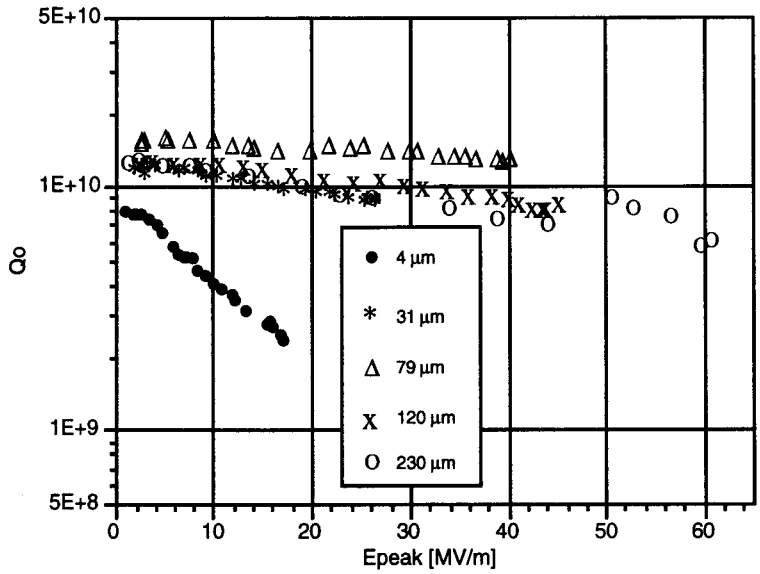


FIGURE 4: $Q_o$ vs. $E_{peak}$ for different amounts of material removal from niobium surface.

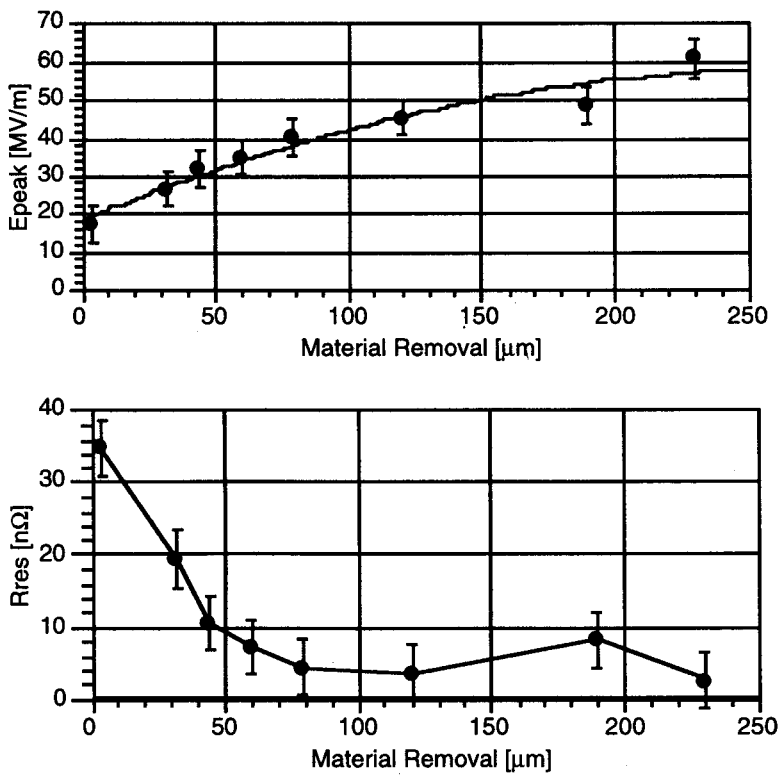


FIGURE 5: Effect of material removal on peak surface electric fields and on residual surface resistance.

### 4.4 *Effect of Cavity Vacuum prior to Cooldown*

A series of 20 experiments with single cell and five cell cavities has been made, during which the cavity was only partially evacuated prior to cooldown and the effect of the frozen-out gas layer on cavity performance was studied. More details of these experiments are given in a separate paper of these proceedings.[15] The results can be summarized as following: "clean" surfaces characterized by the absence of field emission loading are not very sensitive to contamination by residual gases. Above a residual pressure of 1 torr the frozen-out gases caused reversible additional losses. "Contaminated" surfaces however showed increased electronic activity for residual pressures above $10^{-3}$ torr; at pressures below $10^{-4}$ torr no influence on cavity performance was detected. This led to the conclusion that extreme efforts to improve the vacuum conditions in a cavity prior to cooldown for the sole purpose of improving cavity performance do not seem to be necessary. In Figure 6 some data are shown from tests on a single cell cavity.

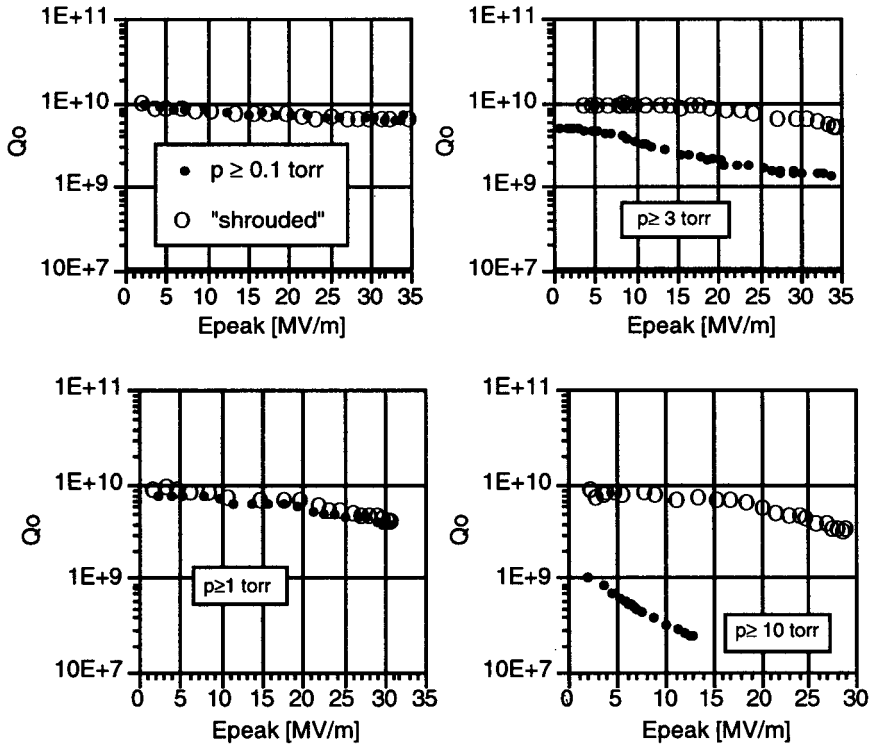


FIGURE 6: Several examples of the performance of a partially evacuated single cell cavity prior to cooldown (• indicates the results at partial pressure, o is after evacuation).

### 4.5 *Effect of Mechanical Stress on the Development of Q-Degradation in Niobium Cavities*

Several years ago the SRF community was shaken by the observation that superconducting cavities made from high purity niobium could significantly degrade in performance when they were kept for longer periods of time at temperatures between 50K and 200K.[16] Many investigations have been conducted in the various laboratories and all experimental evidence supported the intitial hypothesis expressed in[17] of precipitation of a niobium-hydride phase. However the mechanisms involved in dissolution of large amounts of hydrogen into the niobium are less obvious. In[18] it was reported that cavities, which had been heat treated at a moderate temperature of T ≈ 700° C showed again Q-degradation after approximately 50- 60 μm had been chemically removed from the surface even though initially there was no Q-degradation after the heat treatment. On the other hand, a cavity which had been heat treated for several hours at 1400° C, during which the dissolved hydrogen was totally removed as well as any mechanical stresses from the manufacturing process, did not show any degradation even after 4 times the amount of material was

removed from the surface. It had been suggested that mechanical stresses in the material could enhance the pick-up and solution of hydrogen generated during the chemical processing. In order to investigate this hypothesis two cavities were manufactured with different histories: the half cells of cavity 1 were heat treated at 1400° C after forming and prior to welding the cavity, supposedly resulting in a stress-free and hydrogen-free material. For cavity 2 the niobium sheet was heat treated under the same conditions and the stamping of the half cells was done afterwards, introducing some mechanical stresses in the material. The subsequent testing sequence consisted of successive material removal and testing the performance of the cavity at 2 K after a fast cooldown to cryogenic temperature and after a warm-up and "parking" of the cavity at ≈ 100K for ≥ 12 hours. Until now only the experiments with cavity 1 are completed: even after a removal of more than 500 µm, corresponding to a chemical polishing time of nearly 1 hour, no degradation of the Q-value could be seen, even though for the last 100 µm the acid temperature had been raised from room tmeperature to 35° C. Several measurements of this series are collected in Figure 7, showing again the surprisingly good reproducibility of the experimental procedure. The experiments with cavity 2 are not yet completed, but after a removal of approximately 100 µm from the surface this cavity did not show any degradation either until now. It is intended to complete this test series in the near future; it should be possible to draw some kind of a conclusion- be it positive and supporting the hypothesis of stress enhanced hydrogen pick up–or negative, ruling out mechanical stresses as a mechanism for increased hydrogen dissolution.

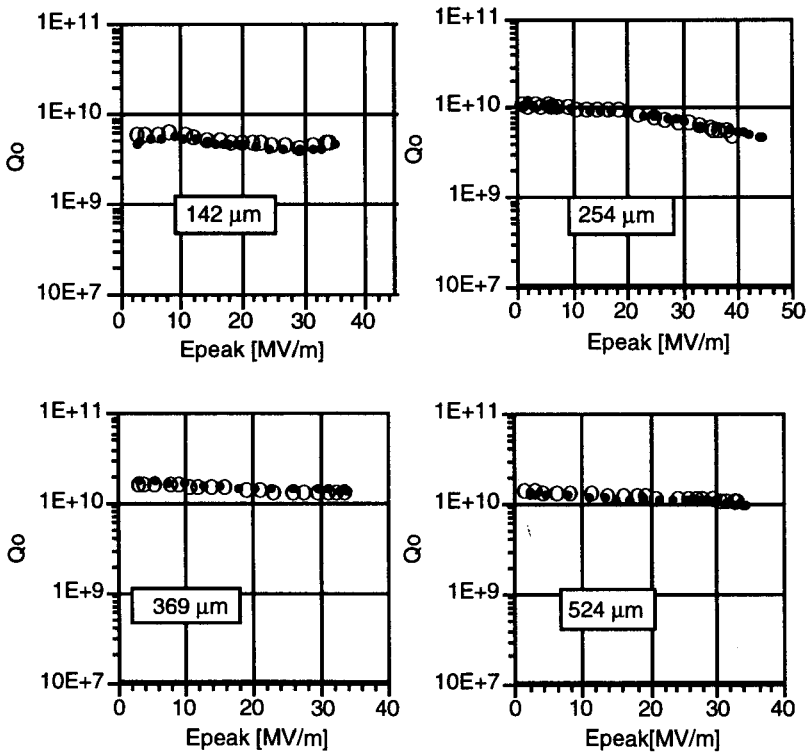


FIGURE 7: $Q_0$ vs. $E_{peak}$ for single cell cavity 1 (no mechanical stresses) after different amounts of material have been chemically removed as indicated. Tests were performed with initially fast cooldown (●) and holding the cavity at ≈ 100K for ≥ 12 hours (O).

### 4.6 *Performance of a nearly "Defect-free" Cavity*

In collaboration with KEK a 1300 MHz single cell cavity optimized for linear collider application was fabricated with standard techniques from RRR ≥ 200 niobium supplied by Tokyo-Denkai. After a removal of ≥ 150 µm from the surface this cavity reached an extremely good performance and the peak surface electric fields could be raised to $E_{peak}$ ≈ 75 MV/m at 1.6 K without field emission loading. Comparison

with thermal model calculations performed at the University of Wuppertal indicated, that in this particular experiment the cavity exhibited a nearly "defect-free" surface. In addition, a Q- value of $Q_0 = 1 \times 10^{11}$ was measured at 1.3 K; this value corresponds to a residual surface resistance of $R_{res} = 2.6\ n\Omega$. More details about these cavity tests and the comparison with thermal model calculations are given in a separate contribution to this workshop.[19]

Figure 8 shows the behavior of the $Q_0$-value as a function of peak surface electric field for three different temperatures. At 2 K and 1.8 K the available rf-power was not sufficient to reach the gradient limit of the cavity, whereas at 1.6 K on oscillatory limit to the high field performance was observed.

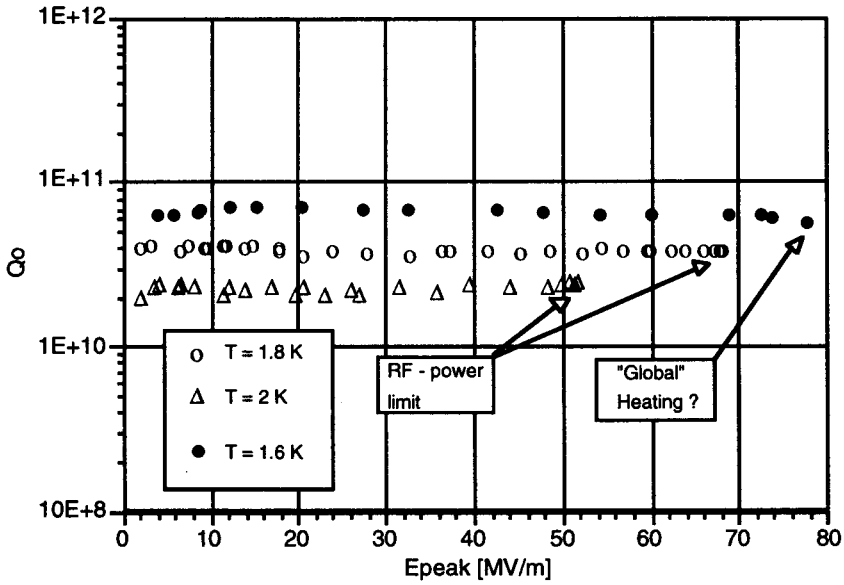


FIGURE 8: $Q_0$ vs. $E_{peak}$ at three different temperatures for a nearly "defect-free" cavity.

### *4.7 Heat Treated Five Cell Cavities*

In order to explore the possible benefits of post purification heat treatments for CEBAF's production cavities several of them were heat treated in the large UHV-furnace of the Kernforschungszentrum Karlsruhe. During the high temperature firing at 1400° C for 4 hours the cavity was surrounded by a 10 mil titanium foil and an additional titanium foil arrangement was placed inside the cavity on axis to enhance the gettering action of the titanium from both sides of the niobium material ("double sided post - purification").

For enhancement of the mechanical stability of the cavity during the heat treatment four niobium rods were mechanically fixed to the cells as supporting elements. This provision was not completely satisfactory as rf-field flatness measurements after the heat treatment showed. The cavity frequency had shifted by several megahertz and the field profile had distorted, demanding a retuning at room temperature .

During the heat treatment niobium samples for thermal conductivity measurements were placed inside the cavities. The measurements indicated that the thermal conductivity of the material had improved by a factor ≥ 2 and the original RRR–value of 250 was slightly over 500.

As is well known titanium is diffusing into the niobium during the heat treatment. Especially diffusion into grain boundaries can penetrate quite deep. This makes it necessary to remove a surface layer in the order of 100 μm after the heat treatment. More recently an improved post purification procedure at lower temperatures has been developed, significantly reducing the diffusion of titanium into the host material.[20] The five cell cavities are typically tested at CEBAF as cavity pairs with all the peripheral parts such as cold rf-windows, HOM-loads and gate valves attached. Since the objective of these tests were aimed at performance improvements of the cavities via material improvements, the heat treated cavities were initially tested without peripheral parts. As it turned out the performance of the cavities was quite good and with this performance baseline the impact of e.g. rf-windows on cavity performance could be investigated.

In Figure 9 the results from 4 heat treated cavities are shown. The degradation of the Q-value for IA 362 is not caused by field emission; the additional resistance represented by the lowered Q-value is proportional to the square of the field and we believe that remaining titanium in grain boundaries might be the cause for the reduction in Q. The encouraging result from these experiments is both the rather high gradient/surface electric fields (in the case of the CEBAF cavity the ratio of peak surface electric field $E_{peak}$ to accelerating gradient $E_{acc}$ is $E_{peak}/E_{acc} = 2.56$) with very little field emission loading and the small spread in the data. Non of the heat treated cavities was limited by a quench; the available rf- power did not permit to reach this limit.

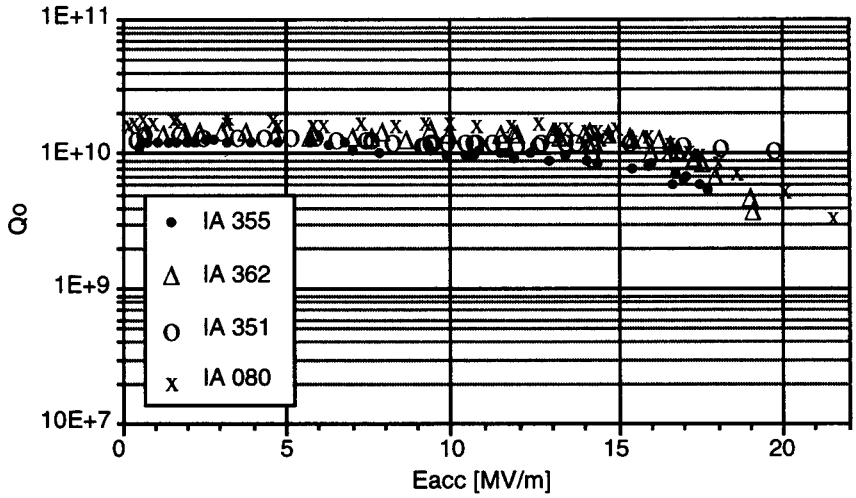


FIGURE 9: Performance of "bare" five cell production cavities after post purification heat treatment at 1400° C. The measurements are taken at T = 2K after removal of approximately 100 μm from the cavity surface ($E_{peak}/E_{acc} = 2.56$).

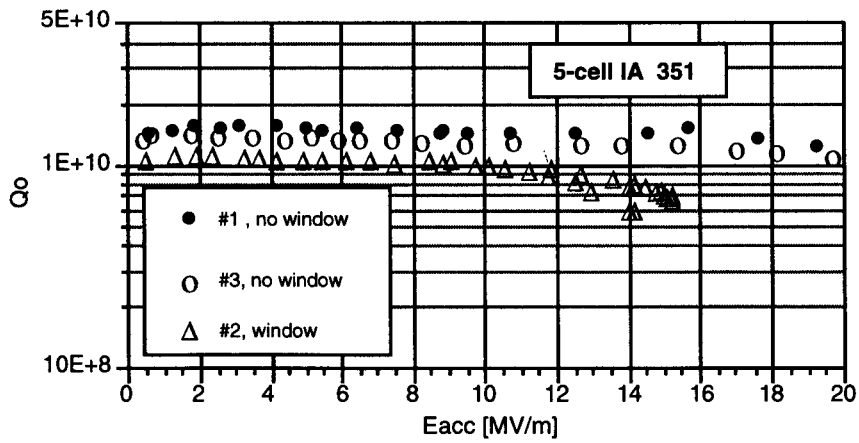


FIGURE 10: Test of heat treated cavity IA 351 without and with ceramic rf-window. The test sequence is indicated in the insert of the figure.

Several ceramic rf-windows were subsequently assembled to some of these cavities. Examples of measurements are shown in Figures 10 and 11, which very clearly indicate a non-negligible impact of this part on cavity performance, most noticable in a lowered Q-value and a reduced gradient. A very significant change has been observed in the Q-values of the other four pass-band modes, which might be an indication of higher than expected losses in the rf-window.

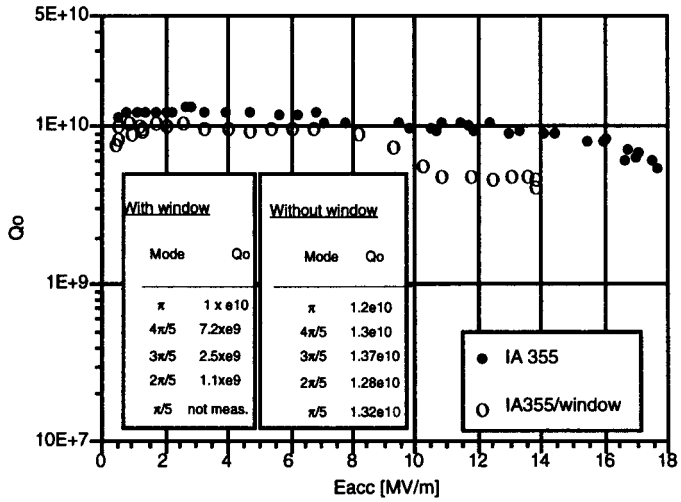


FIGURE 11: Test of a ceramic window on cavity IA 355. The inserts show the significant differences in Q-values of the pass band modes without and with window attachment.

### *4.8 Nb 3Sn - Cavities*

In collaboration with CRYO-ELECTRA and the University of Wuppertal two single cell and a five cell niobium cavities of high thermal conductivity niobium were coated with $Nb_3Sn$ at the University of Wuppertal. The cavities had been fabricated and tested at CEBAF with good performance as niobium cavities and after coating were again tested at CEBAF. Details of the $Nb_3Sn$ technology and the cavity preparation can be found in a separate contribution to these proceedings.[21] The single cell cavities showed extremely encouraging results both in Q-value and in rf- field strenths after high pressure water rinsing. For example, the second cavity had a Q- value of $Q_0 = 2 \times 10^{10}$ at 4.2 K and low field, nearly a factor of 70 higher than niobium at this temperature. At 2 K the quality factor improved to nearly $10^{11}$ corresponding to a residual surface resistance of $R_{res} \approx 2.2$ nΩ. From the temperature dependence of the surface resistance during warm-up of the cavity a critical temperature of $T_c \approx 18$ K was determined. As an example of the performance of these cavities the measured $Q_0$ vs. $E_{peak}$ is plotted in Figure 12.

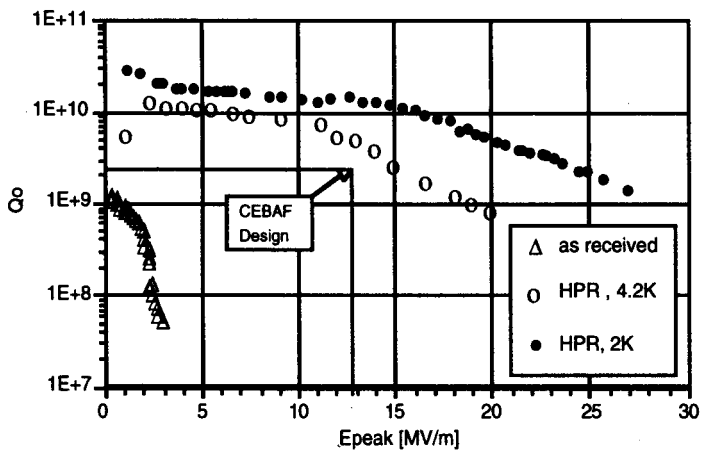


FIGURE 12: Performance of a single cell $Nb_3Sn$ coated cavity. If such performance could be achieved in a multi-cell cavity, CEBAF's design values of Q-value and accelerating gradient would be reached at a temperature of 4.2 K.

## 5. SUMMARY OF EXPERIENCE WITH HIGH PRESSURE ULTRAPURE WATER RINSING

From the experience gained during the last three years involving more than 200 separate tests on niobium and $Nb_3Sn$ cavities, the follwing conclusions can be drawn:

a. High pressure ultrapure water rinsing (HPR) as a final cleaning step after chemical surface treatment resulted in consistant performance of single and multi-cell superconducting cavities.
b. After successive steps of chemical material removal the reproducibility of cavity performance is quite remarkable with only a small spread in data.
c. Application of the same surface treatment procedure to different cavities with subsequent HPR resulted in reliable cavity performance. An estimated > 80% of the cavity tests showed satisfactory performance and no or only insignificant field emission loading for peak surface electric fields $E_{peak} \leq 45$ MV/m.
d. Rinsing of the cavities with reagent grade methanol after HPR and subsequent assembly in a class 100 clean room does not seem to re-contaminate the cavity surfaces.
e. Usually there is no or only very short (≈ min) rf–processing required to achieve the highest fields in a given cavity, indicating a rather "clean" surface.
f. The application of high pressure rinsing resulted not only in reduced field emission loading, but also low residual surface resistances were achieved consistantly.

## 6. PARTICULATE CONTAMINATION OF SURFACES

High pressure ultrapure water rinsing has proven to be a useful tool to overcome the adhesion forces between particulate contamination and substrate for a certain class or size of particles, which might act as electron emitters in high electric rf–fields and limit the performance of superconducting cavities to values below the fundamental limitations of the superconducting material. The question for cavity and accelerator builders arises then how can the level of cleanliness of a superconducting cavity be further improved. In the following it is attempted to give a short overview of available surface cleaning techniques and their applicability to cavity technology.

### *6.1 Adhesion*

Particles stick to surfaces because of adhesion. The interactions include molecular interaction, electrostatic interaction, liquid bridges, double layer repulsion, and chemical bonds. The forces between a substrate and a contaminant are affected by many parameter. To mention a few: the size and shape of the particle, its electric charge, its insulating characteristics, the nature of the substrate, the roughness and electrical charge of the substrate, the hardness of both the particle and substrate, the relative humidity of the environment, the nature of the surrounding medium, the temperature...

There are basically four adhesion forces between a particulate and a solid surface as collected in Table 1. The theoretical background and their physical nature is extensively discussed in the literature and here we will give only a very brief, shallow description. These forces are: van der Waal's forces, capillary forces, electrical double layer forces and electrostatic image forces.

van der Waal's Forces

These intermolecular forces result from the fact that atoms in solids are instantaneous dipols and dispersive interactions between these dipols and neighboring atoms are taking place. Three components of the forces have been identified as dipole-dipole interaction, dipol-non-polar interaction and non-polar interaction.

The interaction is described by a constant–the Hamaker constant A–which is influenced by the particle, the substrate and any medium between both. For a spherical particle of diameter d (1) at a distance of $z_o$ from a flat substrate (2) with a medium (3) in between, the adhesion force is given by $F_{adh} = A_{132} \cdot d / 12 \cdot z_o^2$. $A_{132}$ is the Hamaker constant, which–according to [23]–for example has a value of 1.16 eV for a combination of $Al_2O_3/Al_2O_3$ in water, but increases to 4.68 eV in a vacuum. More data can be found in. [23]

| Type of Force | General Force | Force Equation Reduced for Particulates | Example: 1 μm Glass Particle on Water[23] |
|---|---|---|---|
| Van der Waals | $\frac{\eta \cdot \omega \cdot d}{16\pi z^2}$ | 1.43 x $10^2$d | 1.4 x $10^{-2}$ dyn |
| Cappillary | $2\pi d \cdot \gamma$ | 4.52 x $10^2$d | 4.5 x $w^{-2}$ dyn |
| Electrical double layer | $\frac{\pi \cdot \varepsilon o (A\phi)^2 \cdot d}{2z}$ | 34.8 x d | 0.3 x $w^{-2}$ dyn |
| Electrostatic image force | $\frac{Q^2}{\varepsilon_o \varepsilon d^2}$ | 5 x $10^4$d$^2$ | 0.1 x $10^{-2}$ dyn |

TABLE 1: Adhesion forces between a particle and a solid surface (from[22]) (d = particle diameter, z = distance from surface ~ 4 Å, $\gamma$ = surface tension ~ 73 dyn $cm^{-1}$ in water, $\eta\omega$ = van der Waal's constant ~ 7.2 eV, $\Delta\phi$ = difference in work functions ~ 1 eV. Q = particle charge ~ 10-16C for 1 μm size particle.)

Capillary Forces

Capillary forces are caused by a very thin layer of liquid, e.g. condensation of water vapor, between a particle and a substrate. The meniscus that is formed pulls the components together due to surface tension and reduces the pressure of the liquid. The force is directly proportional to the surface tension of the liquid and depends on the wetting of the particle and substrate. In water the capillary force is largest on hydrophilic surfaces. The force increases with particle size.

Electrical Double Layer Forces [24]

Particles immersed in a liquid medium such as e.g. deionized water will acquire electrical charges. This will attract a compact layer of charges of opposite sign close to the particle, constituting an electrostatic double layer. Further away from the particle a diffuse distribution of ions will provide for electrical neutrality of the suspension. The inner compact layer of adsorbed ions will move with the particle through the liquid, while the ions in the diffuse layer move with the liquid. The boundary between these two regions is the shear plane and the electrical potential at this plane is called the "zeta potential". Substrates immersed in the solution of course are surrounded by the same electrostatic double layer configuration and develop a zeta potential. When the zeta potentials of the particle and the substrate have the same sign, a repulsive force will create a barrier for the diffusion of the particle to the surface. Zeta potentials depend strongly on the pH–value of the solution and vary from positive values at low pH to negative values in basic solutions. Therefore the adhesive forces between a particle and a substrate can be manipulated by the appropriate choice of the liquid medium.

Electrostatic Image Force

This interaction occurs due to the electric charge on particles or the substrate surface. The Coulomb interaction of the charged particle located on a surface is equivalent to an interaction between the particle and its "image". The resulting force is proportional to the square of the charge and inversely proportional to the separation of the particle from the surface (see Table 1).

### 6.2 *Methods For Particle Removal*

The need for improved particle removal techniques has grown tremendously with the advent of higher integration technology in the semiconductor industry and many approches have been taken over the last few years. The list given below might therefore not be a complete representation of the available technologies and might only represent our present state of knowledge. The following cleaning techniques have been reviewed and are shortly summarized here:

High Pressure Jet Cleaning[25]
$CO_2$ - Snow Cleaning[26]
Ice Scrubber Cleaning[27]
Ultraviolet - Ozone Cleaning[28]
Megasonic Cleaning[29]
Isopropyl Alcohol Vapor Displacement[30]
Aerosol Jet Cleaning (supersonic aerosol jet)[31]
Laser Steam Cleaning[32]

High Pressure Jet Cleaning

This method is of course applied in the high pressure rinsing discussed above. It works when the shear stresses applied by a high velocity water jet to a particle exert the adhesion forces holding a particle to a substrate. The drag force $F_d$ applied to a particle of projected frontal area A is proportional to the square of the local fluid velocity v and the fluid density r: $F_d = c \cdot r \cdot v^2/2$ (c = drag coefficient). Since v is proportional to the pressure, it becomes obvious that the removal of smaller particles require much higher pressures, raising concerns that such pressures will damage the substrate. For example the pressure of 80 bar at the high pressure pump in our application of HPR will only remove micron size particle; removal of e.g. 0.5 µm particles would already require a ≈ 5-fold increase in pressure. The fluid dynamics of this cleaning process is treated in detail in.[33]

$CO_2$ - Snow Cleaning

In $CO_2$–snow cleaning a high velocity stream of carbon dioxide gas is directed towards a substrate. The rapid expansion of the liquid or gaseous carbon dioxide stream through a small orifice results in pressure and temperature drops causing nucleation of small liquid droplets and dry ice particles–"snow". Removal of particulates happens when the momentum transfer between the incident dry ice particles and the contaminant overcomes the adhesion forces between particle and substrate. Removal of hydrocarbons by this method is based on the excellent solvent properties of liquid $CO_2$. During impact of the snow particles onto the substrate surface a transient liquid phase is forming at the particle-surface interface. Surface hydrocarbons are absorbed by the liquid $CO_2$, trapped during resolidification and removed, when the snow particle bounces off the substrate.

Ice Scrubber Cleaning

This process is somewhat similar to the $CO_2$–Snow cleaning process with the difference that the $CO_2$ -snow is replaced by fine ice particles of 30 µm to 300 µm produced by spraying ultrapure water into low temperature nitrogen gas. Two mechanisms are considered to be responsible for the removal of even submicron particles: impacting ice particles are smashed into the contaminants, shatter into smaller pieces because they are softer than the substrate and scrub the surface clean under simultaneous application of a carrier gas. In the second mechanism the impacting ice particle melts at the surface and refreezes enclosing and carrying away the contaminating particle. Organic contaminants are removed by the same process after the layers have been broken up mechanically by the impacting ice particles and the thermal contraction changes caused by the cold ice. This process has been applied to a niobium cavity, but system constraints prevented a successful evaluation of the process.[34]

Ultraviolet Ozone Cleaning

This process takes advantage of the ability of ultraviolet light to decompose organic materials such as polymers or hydrocarbons. In addition the process desorbs also gases from substrates. An important variable in the process is the wavelength emitted by the UV source, since only the light which is absorbed can be effective in photochemical changes. Low pressure mercury discharge tubes generate light at 1849 Å, which is absorbed by oxygen and leads to the generation of ozone, and at 2537 Å, which is absorbed by most hydrocarbons and ozone. In the process atomic oxygen is continuously formed leading to oxidation of the contaminants and forming of volatile molecules such as $CO_2$ or water.

Megasonic Cleaning

Megasonic cleaning takes place at frequencies between 0.8 MHz and 1 MHz. These frequencies are very close to the natural oscillation frequencies of the contaminating particles and large oscillation amplitudes can develop. The particles can move far enough from the substrate for wetting to occur beneath it. Whereas the cleaning action in ultrasonic cleaning comes from implosion of air bubbles in the cleaning solution, megasonic cleaning is accomplished by the generation of high pressure waves. In contrast to ultrasonic agitation, megasonic cleaning is quite capable of removing submicron particles down to 0.2 µm.

Since this method works by immersing the contaminated part in a solution with input power densities of 5 - 10 W/cm$^2$, it seems well suited for cleaning of parts with complicated geometries such as cavities. First investigations carried out at KEK gave encouraging results. [11]

Isopropyl Alcohol Vapor Displacement Cleaning

In this method the part to be cleaned is fully immersed in ultrapure water. As the water is drained at a precise rate from the bottom of the tank, submicron filtered warm isopropyl vapor is introduced from the top into the tank to fill the void created by the descending water level. A defined layer of liquid isopropanol forms on top of the descending water as the vapor condenses on contact with the cooler fluid. Interfacial tension between the water and the liquid ispropanol prevents the mixing of both substances.

On slowly withdrawing a hydrophobic part through this gas/liquid interface, interfacial tension is generating forces in opposition to the adhesion forces, stripping the particles away from the substrate. Particles are trapped in the meniscus.

Aerosol Jet Cleaning

In this method a hot stream of nitrogen gas saturated with a chemical vapor and a cold stream of nitrogen gas are mixed, forming ultrafine aerosol droplets by homogeneous nucleation. The aerosol droplets may further grow by coagulation and condensation in the aerosol generation chamber. Subsequently this aerosol expands through a nozzle into a low pressure chamber, where it accelerates to supersonic velocities and impinges onto the substrate to be cleaned. Since the aerosol is generated by a mixing process in the jet cleaning system, a large variety of volatile chemical species can be used to take advantage of their cleaning potential based on the nature of the contamination. The mechanisms attributed to the cleaning action are collision of the high speed droplets with the contaminant particles, scrubbing actions as well as induction of repulsive van der Waal's forces.

Laser Steam Cleaning

This method is based on short pulsed laser irradiation of a surface in connection with the simultaneous deposition of a thin liquid film on the surface of the substrate before the irradiation. Appropriate choice of the laser wavelength, power density and pulse length produces a very efficient heating of the liquid/substrate interface, resulting in superheating and explosive evaporation of the liquid film. The forces generated during this process are by far exceeding the adhesion forces between particle and substrate.

The method has been used successfully to remove particles as small as 0.1 μm.

## 7. CONCLUSION

There might be more advanced cleaning techniques available to promote cleaner surfaces on superconducting cavities. But for many of the techniques described above it might be quite painful to make them work on complicated parts such as cavities. The most promising method seems to be megasonic cleaning, because it is based on an immersion technique. It also has already shown promising results in tests conducted at KEK.

There are concerns however that despite improved levels of cleanliness in initial cavity preparation those surfaces cannot be kept sufficiently clean during subsequent assembly and handling procedures in complex system such as cryomodules. Therefore the same emphasis has to be placed on understanding and avoiding recontamination of clean surfaces. Such efforts are underway in different laboratories.

"In situ" processing techniques such as high peak power processing, which might be able to reverse to some extend recontamination, are important possibilities to achieve the goals for high gradient accelerators.

## ACKNOWLEDGEMENT

We would like to thank all our colleagues who supported this work. Our special thanks go to H. Baumgärtner of the Kernforschungszentrum Karlsruhe for the heat treatment of the cavities, to J. Pauley and R. Afanador for many chemical treatments of cavities, to J. Susta for cryogenic support, to G. Rao for carrying out sample measurements on heat treated niobium, to D. Machie for providing Figure 1 of this note, to L. Turlington and J. Brawley for support in the fabrication of several cavities and to G. Sundeen for editing this paper.

*Supported by DOE contract DE-AC05-84ER40150.

## REFERENCES

1. H. T. Edwards, (1993), *Proc. 6th Workshop on RF Superconductivity,* CEBAF, Newport News, USA, October 1993, 361.
2. E. Mahner, (1993), *Proc. 6th Workshop on RF Superconductivity,* CEBAF, Newport News, USA, October, 1993, 252.
3. N. Pupeter, (1995), invited paper this workshop , to be published.
4. Q. S. Shu, *et al.*, (1989), *Nucl.Instr. and Meth.,* **A 278,** 329.
5. D. Reschke, *et al.,* (1992), *Proc. 3rd European Part. Acc. Conf.,* Berlin, Germany, 1283.
6. J. Graber, *et al.*, (1994), *Nucl.Instr. and Meth.,* **A 350**, 572.
7. C. Crawford, *et al.*, (1995), *Particle Acc.,* **49**, 1.
8. Ph. Bernard, *et al.*, (1992), *Proc. 3rd European Part. Acc. Conf.,* Berlin, Germany, 1269.
9. P. Kneisel, *et al.,* (1993), *Proc. 6th Workshop on RF Superconductivity* CEBAF, Newport News, USA, October 1993, 628.
10. B. Rusnak, *et al.,* (1995), invited paper this workshop , to be published.
11. K. Saito *et al.,* (1995), contibuted paper this workshop, to be published.
12. J. Mammosser, (1993), *Proc. 6th Workshop on RF Superconductivity* CEBAF, Newport News, USA, October, 1993, 33.
13. E. Mahner, *et al.,* (1993), *Proc. 6th Workshop on RF Superconductivity* CEBAF, Newport News, USA, October, 1993, 1085.
14. B. Rusnak, *et al.,* (1992), *1992 Lin. Acc. Conf. Proc. AECL 10728,* Ottawa, Canada, 728.
15. P. Kneisel, (1995), contibuted paper this workshop, to be published.
16. e.g. B. Bonin, R. W.Röth, (1991), *Proc. 5th Workshop on RF Superconductivity* , Hamburg,Germany, 210.
17. R.W. Röth, *et al.,* (1990), *Proc. 32d European Part. Acc. Conf.,* Nice, France, 1097.
18. K. Saito, P. Kneisel, (1992), *Proc. 3rd European Part. Acc. Conf.,* Berlin, Germany, 1031.
19. P. Kneisel, *et al.,* (1995), contibuted paper this workshop, to be published.
20. B. Bonin, *et al.,* (1995), invited paper this workshop , to be published.
21. R. W. Röth et al., (1995), contibuted paper this workshop, to be published.
22. S. Bhattacharya, (1978), *Surface Techn.,* **7**, 413.
23. M. B. Ranade, (1987), *Aerosol Sci. Techn.,* **7**, 161.
24. e.g. R. P. Donovan, *et al.,* (1993), *MRS -Spring-Meeting 1993.*
25. J. Bardina, (1988), in *Particles on Surfaces* edit, by K.L.Mittal, 329.
26. S. A. Hoenig, (1986), *Compressed Air Magazine* , **22.**

27. T. Ohmori, *et al.,* (1989), *Mitsubishi Electric Techn. Report*, **63(11).**
28. J. P. Vig, (1979), in *Surface Contamination* , edit. by K.L.Mittal, 235.
29. S. Shwartzman, *et al.,* (1985), *RCA - Review* **46,** 81.
30. e.g. C. F. McConnell, (1991), *Microcontamination* , Feb., 1991.
31. P. S. Chang, *et al.,* (1993), *MRS -Spring-Meeting 1993.*
32. A. C. Tang, *et al.,* (1992), *Journ. Appl. Phys.* **71(7)**, 3515.
33. R. Gim, *et al.,* (1995), in *Particles on Surfaces* , edit. by K.L.Mittal, 379.
34. Y. Kojima, *private communications.*